Environment, Development and Sustainability
https://doi.org/10.1007/s10668-024-05119-x

Seismic vulnerability analysis of continuous beam bridge based on finite element Method

Jianfeng Li[1,2] · Mengmeng Jin[3] · Junbo Chen[3,4] · Guojun Wang[5] · Yufeng Wang[1] · Huihui Yan[6] · Zucan Weng[7] · Zhigang Huang[8] · Hui Ai[9] · Li Wu[1]

Received: 18 January 2024 / Accepted: 5 June 2024

Abstract
Continuous beam bridges of monopile foundation are commonly used due to its good stress performance, stiffness and beautiful shape. However, scouring will weaken the lateral restraint of soil on pile foundation. It affects the dynamics of the bridge structure and make pile foundation vulnerable to earthquakes. Therefore, it is required to analyze its impacts on continuous beam bridges, especially the seismic vulnerability of the pile foundations. This paper establishes a 3D nonlinear analysis model with OpenSees software, which obtains the probabilistic seismic demand models at three scouring depths by linear regression analysis and incremental dynamic analysis (IDA). It has drawn and analyzed seismic vulnerability curves of pile foundation at three different scouring depths. The influence of scouring around pile foundations on bridge dynamics, seismic response, and vulnerability is obtained. The results indicate that the failure probability of pile foundation decreases with the increase in scouring depth. This demonstrates that scouring around the pile foundation weakens the lateral soil restraint, increasing the natural vibration period of bridge as well as softening the bridge structure. This reduces the maximum seismic response of pile foundation, which is conductive to the seismic resistance of bridge.

Keywords Continuous beam bridge · Finite element · Earthquake vulnerability · Earthquake demand probability model · OpenSees

1 Introduction

Continuous beam bridges are widely used in China for their few joints, good stress performance, simple construction and beautiful shape (Xiang et al., 2019; Cheng & Fu, 2022). However, most continuous beam bridges in mountainous areas and fields with complicated natural environment are easy to be damaged. If natural calamities such as floods or earthquakes happen while the bridge is operating, they would become very susceptible (Liang et al., 2017; Banerjee & Ganesh-Prasad, 2013; Song et al., 2022). Environmental variables may harm continuous beam bridges in farms and hilly regions with complex natural surroundings (Ma et al., 2019; An et al., 2019). The erosion of rainstorm or flood can weaken

Extended author information available on the last page of the article

Published online: 13 June 2024

the foundation (Ma et al., 2021), while high winds and earthquakes can cause sway and collapse (Prakash et al., 2019). Additionally, heavy snowfall may lead to snow accumulation on the bridge, increasing the accidents. This depends on the interaction between snowflakes and engineering surfaces (Guo et al., 2020). During natural disasters such as floods and earthquakes, the bridge becomes more vulnerable. Therefore, considering these factors during design and maintenance is crucial to ensure the safety and longevity of the bridge (Liang et al., 2017; Banerjee & Ganesh-Prasad, 2013; Song et al., 2022). Recent earthquakes in China have severely damaged the country's transport infrastructure, particularly the bridges across major thoroughfares (Huang et al., 2021a; Liu et al., 2023; Zhang & Tien, 2022). Meanwhile, earthquakes may cause flooding and erosion, leading to insufficient bearing capacity of bridges (Das et al., 2022; Huang et al., 2022; Tian et al., 2023). This will cause the bridge piers to overturn during earthquakes, exacerbating the damage to the bridge. According to relevant statistics, during the past three decades, scouring has caused 25% of American bridges to fail, 60% of bridges to collapse (He et al., 2021) and accounting for 20% of the non-seismic reasons for bridge collapse accidents in China (Wang et al., 2022; Xiang et al., 2019).

Scouring leads to less soil around the bridge foundation, causing the exposure of the foundation and lower elevation of overlaying soil. This will weaken the soil constraint on the foundation and affect the dynamics of the bridge structure (Huang et al., 2021b; Xiang et al., 2019; Karimi et al., 2021). Therefore, it is necessary to discuss the impact of scouring around the pile foundation, especially the risk for bridge seismic damage. Currently, seismic vulnerability analysis of bridge is widely used to evaluate the bridge's risk for seismic damage. By examining several seismic waves, it displays the probability-based seismic performance of structures (Hwang & Liu, 2004).

Seismic vulnerability analysis of bridge can be roughly divided into three categories: the expert opinion-based model, the empirical model and the analytical model (Liang et al., 2022). The accuracy of these models depends largely on the quality and accuracy of the data used to develop and validate them. Inaccurate or incomplete data can lead to significant errors in the bridge's seismic vulnerability prediction. Super-hydrophobic sensors play a crucial role in the accuracy of these models. It can give trustworthy and high-quality data even in humid situations, making it an important instrument for data gathering in analyses of the seismic susceptibility of bridges. Furthermore, with the latest developments in their durability against water, it is now possible to ensure that the data collected from super-hydrophobic sensors is accurate and reliable, even in challenging conditions such as severe weather, natural disasters, long-term exposure, and soil erosion (Zhang & Wu, 2019). Among them, the analytical vulnerability analysis model is the most widely used. This is because it depends on theoretical data calculated from finite element model (FEM), without the need to collect a large amount of actual seismic data. Its reliability can be compared to the empirical model (Wang et al., 2021). Although seismic vulnerability analysis of bridge is mature, there is still insufficient research on using this model to analyze the seismic vulnerability curve of bridge under the impact of scouring around the pile foundation. Ye et al. (2007) explored the seismic vulnerability curve of cable-stayed bridge under the impact of scouring around the pile foundation. Ye et al. (2007) designed an analytical vulnerability analysis based on the finite element simulation. By establishing a bridge vulnerability model, Liang et al. (2017) studied the simply supported beam bridge, which reflected the vulnerability of the bridge at different scouring depths under earthquakes, adopting probabilistic seismic demand analy-

sis. However, few studies have focused on the influence of scouring on the seismic vulnerability of continuous beam bridge. Therefore, this research analyzes this type of bridge by establishing a 3D nonlinear analysis model. This model uses the "m" method to simulate the pile soil interaction. It only analyzes the seismic vulnerability curve under the scouring action around the pile foundation for the longitudinal response of the bridge. This study innovatively discusses the impact of scouring on the seismic performance of continuous beam bridges. Then the FEM and IDA are used to reveal the relationship between scouring depth and the seismic vulnerability of bridges, filling the relevant research gap. This study provides scientific support and practical guidance for bridge design and disaster prevention and mitigation.

2 Project overview

2.1 Bridge overview

The bridge is a 4-span, 20 m, and T-shaped pre-stressed height and 12 min width of bridge deck. The cover beams are 1.8 m×1.6 m rectangular beams with a length of 9.8 m. The bridge piers are double column piers with fixed bearings, with diameter 1.6 m and pier height 10.8 m. The longitudinal bars adopt45 HRB335 φ28 and stirrups take HPB300 φ8 with a spacing of 150 mm. The tie-beams are 1 m×1.2 m rectangular beams. The foundation is bored pile foundation, 2 min pile diameter and 23 m in pile length. Its longitudinal bars adopt 60 HRB335 φ28 and its stirrups use HPB300 φ8 with a spacing of 150 mm. The double-column piers, covering beams, tie beams and pile foundations, are made of C30 concrete continuous beam (Fig. 1). Each span is composed of five C45 concrete and T-shaped beams, with a beam length of 1.5 m.

The fixed bearing and sliding bearing of bridge are GYZ φ450×99 laminated rubber bearing and GYZF4 φ350×87teafluoroethylene sliding-plate bearing, respectively.

2.2 Determination of the scouring depth around the pile foundation

There are three common calculation methods of maximum local scouring depth at home and abroad (Liu & Lu, 2019; Jiang et al., 2021):
Breusers method:

$$\frac{H}{D} = k \tanh(h/D) \tag{1}$$

Sumer method:

$$\frac{H}{D} = 1.3 \tag{2}$$

CSU/HEC-18 method:

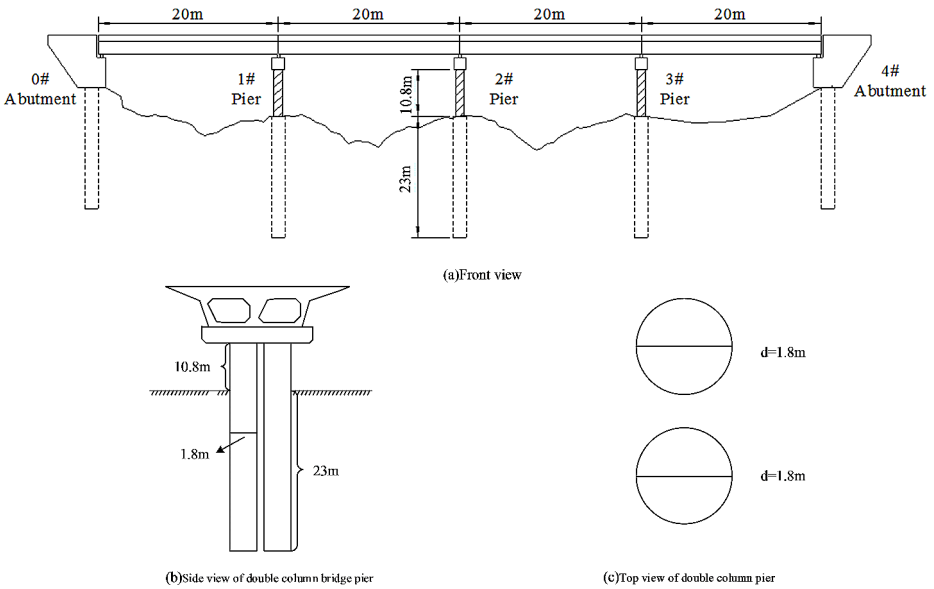

Fig. 1 Overall layout of bridge

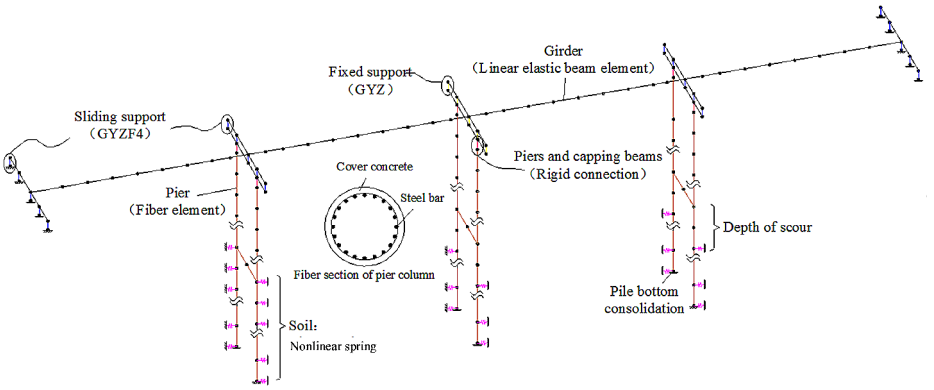

Fig. 2 Finite element model of bridge

$$\frac{H}{D} = 2G_1G_2G_3G_4(h/D)^{0.35}Fr^{0.43}, Fr = \frac{V}{(gh)^{0.5}} \tag{3}$$

In Eq. (1), H represents the scouring depth. D is the pile foundation diameter, at 2 m. k represents the coefficient. k is often used to adjust the prediction of scouring depth, taking into account factors such as the dynamic characteristics of the river, the material of the river bed, and the shape and size of the bridge pile foundation. k=2 is widely used in engineering practice. It is considered that it can reasonably reflect many influencing factors in the scouring process. h is the water depth, taking 10 m. Based on these parameters, the scouring depth calculated by Breusers method is 4.0 m. Secondly, the Sumerian method is used to

calculate the scouring depth. Since the diameter of pile foundation is known to be 2 m, the scouring depth is relatively simple to calculate, and the scouring depth can be obtained as 2.6 m. Finally, the scouring depth is calculated by CSU/HEC-18 method. In Eq. (3), G1, G2, G3 and G4 are all uncertain coefficients, and their values are uniformly 1.0 in the case of cylindrical piles. These coefficients are often used to adjust the prediction accuracy of the scouring equation to suit different river environments and pile foundation shapes. Since the pile foundation is cylindrical and there are no special bed formations or flow conditions to be considered, it is reasonable to choose these coefficients of 1.0. In addition, Fr in Eq. (3) represents the Froud coefficient, which is calculated according to velocity V and depth h, as well as gravitational acceleration g. In the calculation, the velocity V is set at 1.1 m/s, the depth h is set at 10 m, and the acceleration g is set at 9.8 m/s^2. These values are based on actual engineering conditions and site survey data. Velocity and water depth, in particular, are critical to the scouring depth calculation, so these values are determined based on field measurements and river dynamics models. Therefore, the scouring depth of 2.6 m is obtained by CSU/HEC-18 method under the given water depth, velocity and gravitational acceleration. The values of the above parameters are widely used in engineering practice. It is considered that they can reasonably reflect the various influencing factors in the scouring process, so as to provide a reliable basis for the scouring depth calculation.

By comparing the above three methods, it is concluded that the maximum scouring depth of continuous beam bridge is 4.0 m. In order to analyze the impact of scour on pile foundation more comprehensively, the scour conditions around pile foundation are further subdivided into three conditions: no scouring, scouring depth of 2 m and scouring depth of 4 m. This classification helps to more accurately evaluate the stability and safety of pile foundations under different scouring conditions.

3 Analysis model establishment

3.1 FEM

This paper builds a FEM of continuous beam bridge with ASDEA STKO for OpenSEES software (Fig. 2).

In order to describe the FEM more comprehensively, more detailed parameter values are provided below. The parameters of the main beam and cover beam are as follows. For the concrete used in the main beam and cover beam, the elastic modulus E is 30 GPa. The section size of the main beam may be T-shaped or rectangular according to the design, the specific size is as described in the article, the section size of the cover beam is 1.8 m×1.6 m. The mass density of concrete ρ is about 2400 kg/m^3. The parameters of the tie beam and pile foundation are as follows. The compressive strength fc' of the concrete material is 40 MPa. The elastic modulus E is also 30 GPa. The value of Poisson's ratio ν is 0.2. The parameters of steel material properties are as follows. The yield strength (fy) is set to 400 MPa. The elastic modulus of steel is set to 200 GPa. The elongation is determined according to different reinforcement types. The pile-soil interaction parameters are as follows. The proportional coefficient k of foundation coefficient varying with depth is 12 MN/m^4. In addition, the damping ratio of the structure is set to 0.05. The pre-processor aspect of this software provides convenient GUI operations. The pre-processor relies on the HDF-5 database to

present various displacements, stresses, and strains in the post-processing, thereby constructing a FEM of the bridge. The main beams and cover beams are simulated with elastic beam elements. The main beam weight and the second phase constant loads are converted into node masses. In the research of Farahmand-Tabar and Barghian (2020), it is found that the bridge substructure is prone to damage under seismic action. Therefore, tie beams and pile foundations are simulated with non-linear fiber elements. Concrete 02 and Steel 02 are adopted as the material of fiber elements, respectively. Moreover, for the pile-soil interaction, the equivalent linear spring is applied to pile foundation element nodes, and the pile bottom is consolidated (Dang et al., 2023; Liang et al., 2019; Shen, 2020; Wu et al., 2022). The soil is distributed around the pile foundation, so two nonlinear springs are installed at the node of the pile foundation unit. They are nonlinear springs in the x direction and nonlinear springs in the y direction, respectively. The stiffness of nonlinear springs is calculated with the "m" method, with the Equation as follows:

$$k = m_i b z_i h_i \tag{4}$$

In Eq. (4), m_i is the proportional coefficient (MN/m^4) of the variation of the foundation coefficient with depth. In this study, the foundation is mainly composed of medium sand, so the m_i is 12 MN/m^4. b denotes the calculation width of pile. z_i shows the distance between the soil center and the ground (or scouring line). h_i is the thickness of soil. m_i and b are values in the Code for Design of Ground Base and Foundation of Highway Bridges and Culverts (JTG 3363−2019) (Li et al., 2012).

3.2 Ground motion input

In this paper, 10 representative seismic records from PEER strong earthquake database are carefully selected from different seismic events and geographical locations to ensure their diversity and universality. These include historical records of famous seismic events such as the Northridge earthquake and the Loma Prieta earthquake, which not only have different magnitudes and epicentral distances, but also cover various site conditions and seismic wave characteristics. The reason for choosing these records is that they can comprehensively reflect the response of the structure under different seismic actions, so as to provide more accurate data support for subsequent seismic design and performance evaluation. The surface peak ground acceleration (PGA) is used as the seismic intensity index and normalized to 0.1–1.0 g by IDA method to generate sufficient sample calculation data. After 100 normalized ground motion samples are input into the analysis model, an in-depth nonlinear dynamic analysis is carried out to evaluate the seismic performance of the structure more accurately. This rigorous selection and analysis process is essential to ensure the stability and safety of the building structure.

3.3 Bridge dynamic characteristics analysis

Through the mode analysis of bridges, the First-Step-Fifth-Step natural vibration periods of the bridge under three scouring conditions are obtained (Table 1).

According to Table 1, the erosion around the pile foundation gradually increases the natural vibration period of the bridge, indicating that the overall stiffness of bridge structure

Table 1 The first-step-fifth-step natural vibration periods of bridge under three scouring conditions

Scouring depth (m)	Natural vibration period (s)				
	T_1	T_2	T_3	T_4	T_5
0	1.61	1.30	1.14	0.38	0.38
2	1.70	1.34	1.15	0.41	0.41
4	1.77	1.37	1.16	0.44	0.44

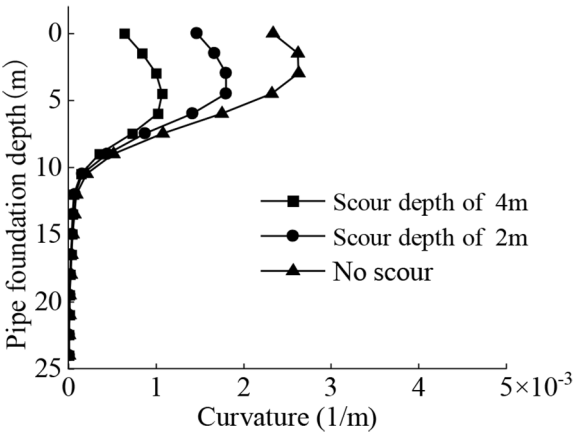

Fig. 3 Changes of maximum curvature of pile foundation under three scouring depth

is reduced. The first step natural vibration period increases from 1.61 s without scouring to 1.77 s at a scouring depth of 4 m, an increase of 9.9%. The second step natural vibration period increases from 1.3 s without scouring to 1.37 s at a scouring depth of 4 m, an increase of 5.4%.

3.4 Bridge seismic response analysis

Five ground motions in Sect. 3.2 are randomly selected to analyze the seismic response of pile foundation at PGA = 0.6 g (Fig. 3). Figure 3 illustrates the absolute maximum curvature of the pile foundation below the soil surface in five records. After the scouring, the maximum curvature of pile foundation moves down due to the lower level of the soil surface. In a word, the maximum curvature of pile foundation decreases with the increase of scouring depth.

4 Analysis of bridge seismic vulnerability

4.1 Seismic vulnerability function

Bridge seismic vulnerability refers to the conditional probability that the structural response (S_d) reaches or exceeds the structural carrying capacity (S_c) of the bridge in different PGA. The Equation is as follows:

$$P_f = P[\frac{S_d}{S_c} \geq 1] \tag{5}$$

S_d and S_c are supposed to follow the logarithmic normal distribution. Then the Eq. (5) can be written as:

$$P_f = \Phi[\frac{\ln(\frac{S_d}{S_c})}{\sqrt{{\beta_c}^2 + {\beta_d}^2}}] \tag{6}$$

According to HAZUS99 (Konstantakopoulos et al., 2012), when PGA is used as the independent variable, $\sqrt{{\beta_c}^2 + {\beta_d}^2}$ takes 0.5.

According to Cornell's recommendations (Li et al., 2019), the relationship between structural response and PGA can be expressed as:

$$\ln(S_d) = k \cdot \ln(PGA) + b \tag{7}$$

Equation (7) is the model of probabilistic seismic demand. It can be obtained through the regression analysis of bridge seismic response data. Equation (6) can be converted into:

$$P_f = \Phi[\frac{k \cdot \ln(PGA) + b - \ln(\mu_c)}{0.5}] \tag{8}$$

In Eq. (8), P_f represents the probability that the structural response of the bridge reaches or exceeds its structural bearing capacity under the given ground peak acceleration condition. This is a key indicator of how vulnerable a bridge is to earthquake damage. By calculating P_f, the safety and reliability of bridges under different PGA conditions can be evaluated, which provides an important basis for seismic design and reinforcement of Bridges. Φ is the cumulative distribution function of the standard normal distribution. This function provides a way to convert the ratio between the structural response of a bridge and its carrying capacity into a probability value, which is convenient for researchers to intuitively understand the safety status of the bridge. *k* and *b* are derived from probabilistic seismic demand models, which represent the linear relationship between structural response and PGA. *k* is the slope, representing the increase of the structural response when PGA increases by one unit. *b* is the intercept, which represents the predicted value of the structural response when PGA is 0. These two parameters can be obtained by regression analysis of bridge seismic response data. By determining these two parameters through regression analysis, a quantitative relationship between the bridge structural response and PGA is established, and then the structural response under different PGA conditions is predicted. μ_c represents the average bearing capacity of multiple bridge structures. This value is obtained by statistical analysis of the carrying capacity of multiple Bridges. In addition, μ_c can take different values to represent different damage states of the bridge, and its value range is usually between 10 and 30. μ_c is an important parameter to evaluate the bridge vulnerability. By comparing the structural response to μ_c, the researchers can determine the bridge's safety margin under different PGA conditions. At the same time, by adjusting the value of μ_c, the bridge vulnerability under different damage states can be simulated. PGA is an important indicator to

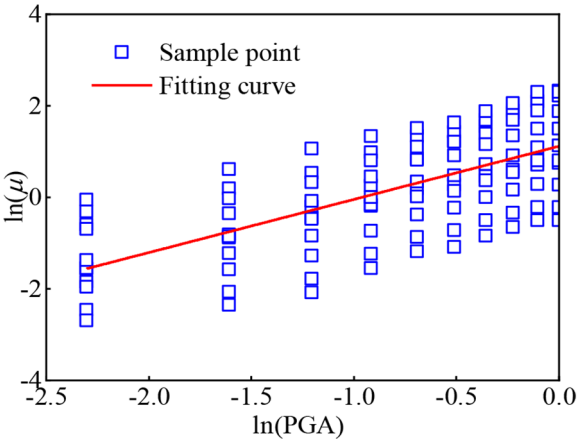

Fig. 4 Probabilistic seismic model for pile foundations with a scouring depth of 2 m

Table 2 Values of k, b and R^2 under three scouring impacts

Scouring depth (m)	k	b	R^2
0	1.1620	1.1168	0.9845
2	0.9384	0.7958	0.9863
4	0.8767	0.6216	0.9964

describe the intensity of the earthquake, indicating the maximum acceleration of the object on the ground in the earthquake. In earthquake engineering, the PGA is an important parameter for evaluating earthquake intensity. The size of bridge PGA directly affects the structural response and bridge vulnerability. The bridge vulnerability under different conditions PGA can provide an important basis for seismic design and strengthening of bridge.

This paper selects the curvature ductility ratio as the damage state index of pile foundation. There are four different types of pile foundation damage: minor damage, moderate damage, serious damage and complete damage. The critical values of curvature ductility ratio of each damage state are 1, 1.14, 2.23 and 4.35, respectively (Ehsan et al., 2020).

4.2 Seismic vulnerability curve of bridge under three scouring depths

The probabilistic seismic demand model of pile foundation at three scouring depths can be obtained through linear regression of the maximum curvature of the pile foundation. PGA is the independent variable. This paper presents the model of probabilistic seismic demand at the scouring depth of 2 m (Fig. 4). The coefficients under three scouring impacts are shown in Table 2.

The seismic vulnerability curve can be calculated according to Table 2 and Eq. (8) (Fig. 5, 6 and 7).

From Fig. 5, 6 and 7, after scouring around the pile foundation, the failure probability of pile foundation under each damage state increases significantly with the increase of PGA. When PGA≤0.1 g, the failure probability increases very little, indicating that the pile foundation may be in an elastic state. When 0.1 g<PGA≤0.6 g, the failure probability increases rapidly, illustrating that the pile foundation may enter the elastoplastic stage.

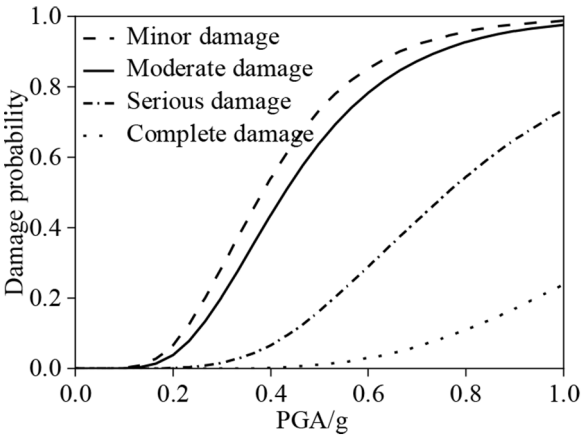

Fig. 5 Seismic vulnerability curve of pile foundation under no scouring condition

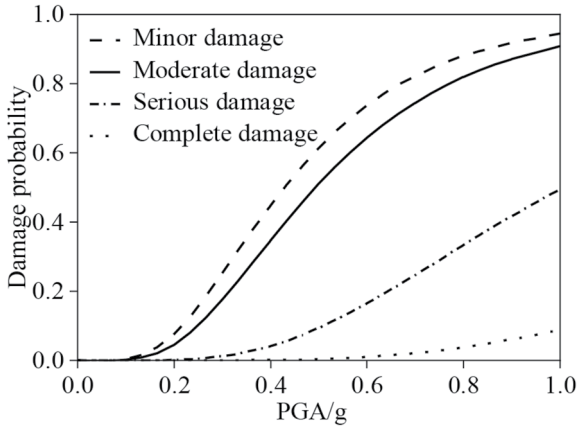

Fig. 6 Seismic vulnerability curve of pile foundation at the scouring depth of 2 m

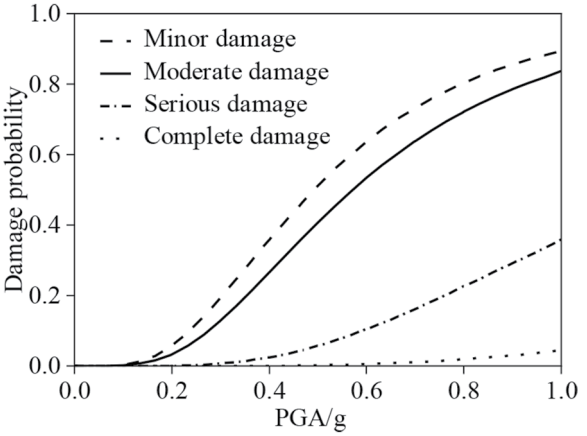

Fig. 7 Seismic vulnerability curve of pile foundation at the scouring depth of 4 m

When PGA>0.6 g, the failure probability is high, but its increase rate slows down, demonstrating that the pile foundation may be in a plastic state. The pile foundation consumes part of the energy with a severe deformation (He et al., 2020).

It is necessary to compare the changing pattern of the seismic vulnerability curve of pile foundation under three scouring depths. Consequently, this paper presents the seismic vulnerability curves of pile foundation at three scouring depths under four damage states (Fig. 8).

According to Fig. 8, the failure probability of pile foundation decreases with the increase in scouring depth under four damage states, such as in the moderate damage state. When PGA=0.6 g, the probability of pile foundation failure decreases from 78.3% without scouring to 53.3% at a scouring depth of 4 m, with a decrease of 25%. It indicates that scouring around the pile foundation facilitates the earthquake resistance of bridge. This is because the scouring around the pile foundation weakens the lateral soil restraint on pile foundation, increasing the pier height and decreasing the overall stiffness of bridge structure. Therefore, it softens the bridge structure. The result verifies that scouring increases the period of bridge structure and reduces the overall stiffness of bridge structure in Sect. 4. In order to verify the correctness of the above results, the research also carries out different verification work. Firstly, different seismic wave inputs are used for multiple analyses to ensure the stability and reliability of the results. These seismic waves include different magnitudes, epicentre distances and site conditions to more fully assess the bridge's response to differ-

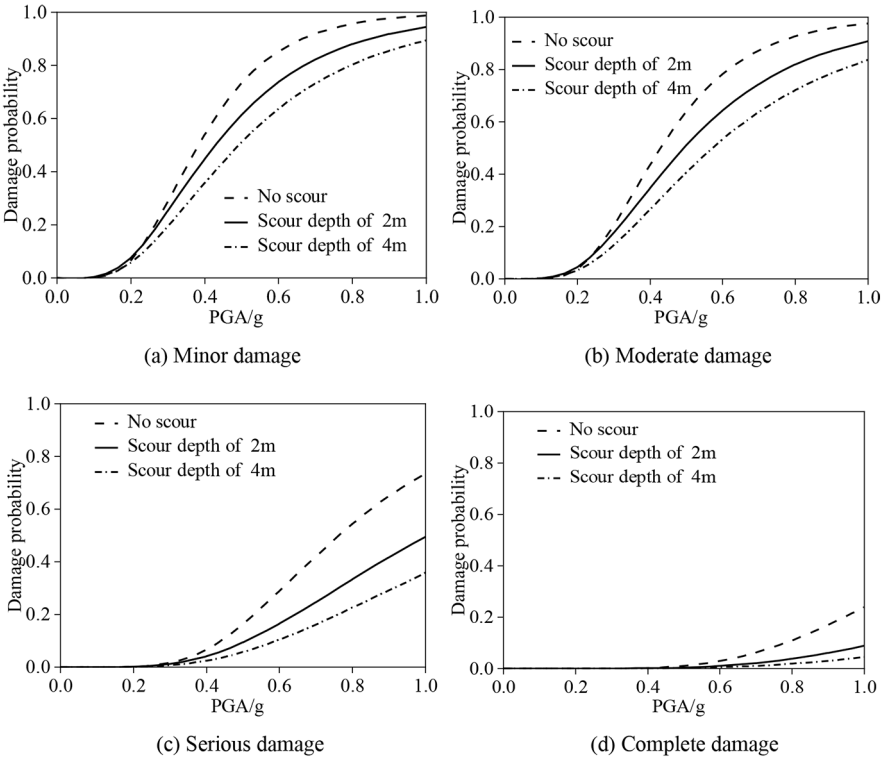

Fig. 8 Seismic vulnerability curve of pile foundation at three scouring depths under four damage states

ent earthquakes. Through comparative analysis, it is found that the seismic response and vulnerability trend of the bridge are consistent under different seismic waves, which further confirms the authenticity of the research results. Secondly, other independent numerical analysis software are used for cross-validation. By inputting the same bridge model and ground motion data, the seismic response and vulnerability results calculated by different software are compared. The verification results show that the conclusions obtained by different software are basically consistent within the error range, which further enhances the credibility of the research results. In this study, the influence of seismic wave characteristics on the structural response of the bridge is considered in the seismic vulnerability analysis of the bridge. Because of the non-stationary of seismic waves, including the variation of amplitude, frequency and duration, the seismic response of bridges is significantly affected. For example, it has been found that some seismic waves may contain rich long-period components, which are more likely to excite the low-frequency modes, thereby increasing the displacement response and stress of structures (Wei et al., 2024a). This study emphasizes the complexity of seismic wave characteristics on bridge response and further confirms the necessity of considering the effect of seismic wave characteristics.

In addition, studies have found that if isolation devices, such as self-centering bearings, are used in bridges, positive effects are usually produced (Wei et al., 2024b). These isolation devices can effectively reduce the transmission of seismic energy to the bridge structure, thereby reducing the seismic response of the structure and potential damage risk. Specifically, isolation devices such as self-centering bearings can allow the bridge structure to experience a certain displacement when an earthquake occurs, thereby consuming seismic energy and reducing the impact on the structure. In addition, other studies have found that bridges using isolation devices have significantly better seismic performance than those without isolation devices (Fu & Wei, 2024). Therefore, the seismic effect can be improved by adding appropriate isolation devices in the future.

5 Conclusions

In order to improve the seismic performance of bridges, finite element modeling and seismic response analysis were proposed to explore the influence of scouring depth on the seismic response and vulnerability of bridges. Through finite element modeling and seismic response analysis, the increase of scouring depth led to the decrease of the overall stiffness of the bridge, and then affected the seismic response of the bridge. The seismic vulnerability curve showed that the failure probability of pile foundation decreased with the increase of erosion depth under the same ground motion intensity. This result may be related to the weakening of lateral soil constraint and the increase of pier height caused by erosion, which combined to soften the bridge structure. In addition, the isolation device could improve the seismic effect, and the appropriate isolation device could effectively improve the seismic effect. In conclusion, this study reveals the important influence of scouring depth on seismic vulnerability of bridges, providing a new perspective for seismic design of bridges. However, there are some shortcomings in the study, such as the impact of different soil types, water flow speed and other complex factors on the erosion and seismic performance of the bridge, which will be the future research direction.

Abbreviations

IDA Incremental Dynamic Analysis
FEM Finite Element Model
PEER Pacific Earthquake Engineering Research
PGA Peak Ground Acceleration

Funding No funding was received to assist with the preparation of this manuscript.

Data availability Some or all data, models, or code that support the findings of this study are available from the corresponding author upon reasonable request.

Declarations

Conflict of interest The authors have no competing interests to declare that are relevant to the content of this article.

References

An, Y., Chatzi, E., Sim, S., Laflamme, S., Blachowski, B., & Ou, J. (2019). Recent progress and future trends on damage identification methods for bridge structures. *Structural Control and Health Monitoring*, *26*(10), 1–30. https://doi.org/10.1002/stc.2416.

Banerjee, S., & Ganesh-Prasad, G. (2013). Seismic risk assessment of reinforced concrete bridges in flood–prone regions. *Structure and Infrastructure Engineering*, *9*(9), 952–968. https://doi.org/10.1080/15732479.2011.649292.

Cheng, Y., & Fu, L. (2022). Nonlinear seismic inversion by physics–informed Caianiello convolutional neural networks for overpressure prediction of source rocks in the offshore Xihu depression, East China. *Journal of Petroleum Science and Engineering*, *215*, 110654. https://doi.org/10.1016/j.petrol.2022.110654.

Dang, P., Cui, J., Liu, Q., & Li, Y. (2023). Influence of source uncertainty on stochastic ground motion simulation: A case study of the 2022 mw 6.6 Luding, China, earthquake. *Stochastic Environmental Research and Risk Assessment*. https://doi.org/10.1007/s00477-023-02427-y.

Das, S., Halder, K., & Chakraborty, D. (2022). Seismic bearing capacity of shallow embedded strip footing on rock slopes. *Geomechanics and Engineering*, *30*(2), 123–138. https://doi.org/10.12989/gae.2022.30.2.123.

Ehsan, B., Ali, N., Abdelmalek, B., Yannis, D., Shima, Z., & Louis, K. (2020). Load recovery mechanism of arching within piled embankments using discrete element method and small scale tests. *Powder Technology*, *359*, 59–75. https://doi.org/10.1155/2021/5518233.

Farahmand-Tabar, S., & Barghian, M. (2020). Seismic assessment of a cable–stayed arch bridge under three–component orthotropic earthquake excitation. *Advances in Structural Engineering*, *24*(2), 227–242. https://doi.org/10.1177/1369433220948756.

Fu, Y., & Wei, B. (2024). A two-dimensional friction-decoupling method based on numerical integration method and momentum theorem. *Engineering Structures*, *301*, 117323. https://doi.org/117323.

Guo, Q., Feng, L., Zhang, R., & Yin, H. (2020). Study of damage identification for bridges based on deep belief network. *Advances in Structural Engineering*, *23*(8), 1562–1572. https://doi.org/10.1177/1369433219898058.

He, L. G., Hung, H. H., Chuang, C. Y., & Huang, C. W. (2020). Seismic assessments for scoured bridges with pile foundations. *Engineering Structures*, *211*(15), 1–10. https://doi.org/10.1016/j.engstruct.2020.110454.

He, H. F., Wei, K., & He, C. (2021). Lateral seismic vulnerability analysis of continuous girder bridges on the Sichuan Tibet line considering the impact of scouring. *Journal of Disaster Prevention and Mitigation Engineering*, (3), 441–447. https://doi.org/10.13409/j.cnki.jdpme.201904083.

Huang, S., Huang, M., & Lyu, Y. (2021a). Seismic performance analysis of a wind turbine with a monopile foundation affected by sea ice based on a simple numerical method. *Engineering Applications of Computational Fluid Mechanics*, *15*(1), 1113–1133. https://doi.org/10.1080/19942060.2021.1939790.

Huang, S., Lyu, Y., Sha, H., & Xiu, L. (2021b). Seismic performance assessment of unsaturated soil slope in different groundwater levels. *Landslides*, *18*(8), 2813–2833. https://doi.org/10.1007/s10346-021-01674-w.

Huang, H., Li, M., Yuan, Y., & Bai, H. (2022). Theoretical analysis on the lateral drift of precast concrete frame with replaceable artificial controllable plastic hinges. *Journal of Building Engineering*, *62*, 105386. https://doi.org/10.1016/j.jobe.2022.105386.

Hwang, H., & Liu, J. B. (2004). Vulnerability analysis of reinforced concrete bridge structure under earthquake. *Journal of Civil Engineering*, *37*(6), 47–51. https://doi.org/10.15951/j.tmgcxb.2004.06.009.

Jiang, H., Gu, Q., Huang, L., Li, C., Meng, X. F., & Ma, X. Y. (2021). Seismic vulnerability analysis of offshore cable-stayed bridges considering the time-varying deterioration effect of chloride ion erosion. *Journal of Southeast University (Natural Science Edition)*, *51*(1), 38–45. https://doi.org/10.3969/j.issn.1001-0505.2021.01.006.

Karimi, J., Asadizadeh, M., Hossaini, M. F., Nowak, S., & Sherizadeh, T. (2021). Compressive strength of flawed cylindrical specimens subjected to axial loading. *Geomechanics and Engineering*, *27*(1), 89–101. https://doi.org/10.12989/gae.2021.27.1.089.

Konstantakopoulos, T. G., Raftoyiannis, I. G., & Michaltsos, G. T. (2012). Suspended bridges subjected to earthquake and moving loads. *Engineering Structures*, *45*, 223–237. https://doi.org/10.1016/j.engstruct.2012.06.044.

Li, L. F., Wu, W. P., Huang, J. M., & Wang, L. H. (2012). Study on vulnerability of medium span RC continuous beam bridge system under earthquake. *Journal of Civil Engineering*, *45*(10), 160–168. https://doi.org/10.15951/j.tmgcxb.2012.10.005.

Li, J. W., Gong, L., Xu, L. Q., & Tao, Y. (2019). Influence of pile foundation scouring on seismic response of offshore long-span cable-stayed bridge. *Journal of Xihua University (Natural Science Edition)*, *38*(5), 12–18. https://doi.org/10.3969/j.issn.1673-159X.2019.05.002.

Liang, F. Y., Liu, B., & Li, J. R. (2017). Seismic fragility analysis of bridge pile foundation considering scour effect. *China Earthquake Engineering Journal*, *39*(1), 13–19. https://doi.org/10.3969/j.issn.1013-0019.2017.01.0013.

Liang, Y., Yan, J. L., Niu, H., & Li, J. (2019). Time varying seismic vulnerability analysis of offshore piers considering the effect of main aftershocks. *Journal of Seismic Engineering*, *41*(4), 887–894. https://doi.org/10.3969/j.issn.1000-0844.2019.04.887.

Liang, Y., Zhao, F., Luo, J., & Chen, P. (2022). Study on time-varying seismic vulnerability and analysis of ECC-RC composite piers using high strength reinforcement bars in offshore environment. *Earthquake Engineering and Engineering Vibration*, *21*(4), 1035–1051. https://doi.org/10.1007/s11803-022-2123-2.

Liu, Y. G., & Lu, L. (2019). Influence of scouring on seismic response of pile foundation of continuous beam bridge. *Sichuan Architectural Science Research*, *45*(1), 17–21. https://doi.org/10.19794/j.cnki.1008-1933.2019.01.004.

Liu, C., Peng, Z., Cui, J., Huang, X., Li, Y., & Chen, W. (2023). Development of crack and damage in shield tunnel lining under seismic loading: Refined 3D finite element modeling and analyses. *Thin-Walled Structures*, *185*, 110647. https://doi.org/10.1016/j.tws.2023.110647.

Ma, L., Zhang, W., Han, W. S., & Liu, J. X. (2019). Determining the dynamic amplification factor of multi-span continuous box girder bridges in highways using vehicle-bridge interaction analyses. *Engineering Structures*, *181*, 47–59. https://doi.org/10.1016/j.engstruct.2018.11.059.

Ma, L., Zhang, W., Cai, S., & Li, S. (2021). The dynamic amplification factors for continuous beam bridges along high-speed railways. *Advances in Structural Engineering*, *24*(11), 2542–2554. https://doi.org/10.1177/13694332211003288.

Prakash, V., Kumawat, S., & Singh, P. (2019). Design and analysis of full and half mode substrate integrated waveguide planar leaky wave antenna with continuous beam scanning in X-Ku band. *Frequenz*, *73*(5–6), 171–178. https://doi.org/10.1515/freq-2018-0212.

Shen, H. J. (2020). *Vulnerability analysis of high–speed railway continuous girder bridge under near–field earthquake*. Master Thesis, China, Jiangsu: Nanjing, Southeast University, 75p.

Song, S. T., Hu, T. F., & Chiou, D. J. (2022). Influence of riverbed scour on the performance of bridges subjected to lateral seismic loads. *Journal of Earthquake Engineering*, *26*(5), 2251–2282. https://doi.org/10.1080/13632469.2020.1758851.

Tian, L., Li, M., Li, L., Li, D., & Bai, C. (2023). Novel joint for improving the collapse resistance of steel frame structures in column-loss scenarios. *Thin-Walled Structures*, *182*, 110219. https://doi.org/10.1016/j.tws.2022.110219.

Wang, D. B., Xia, Q., Sun, Z. G., Wang, D. S., & Liu, D. (2021). Seismic fragility comparative research of sea–crossing bridges with scour conditions under onshore and offshore ground motions. *Advanced Engineering Sciences*, *53*(5), 127–137. https://doi.org/10.15961/j.jsuese.202000910.

Wang, N., Xing, G., Zhu, T., Zhou, H., & Shi, Y. (2022). Propagating seismic waves in VTI attenuating media using fractional viscoelastic wave equation. *Journal of Geophysical Research: Solid Earth*, *127*, e2021JB023280. https://doi.org/10.1029/2021JB023280.

Wei, B., Lu, A., Jiang, L., Yan, L., & Sun, Z. (2024a). Effect of ground motion time–frequency non-stationarity on seismic response of high-speed railway simply supported bridge based on wavelet packet transform. *International Journal of Structural Stability and Dynamics*, 2450247. https://doi.org/10.1142/S021945542450247X.

Wei, B., Tan, H., Jiang, L., Xiao, B., & Lu, A. (2024b). Shaking table test of the seismic performance for railway simply-supported girder bridge isolated by self-centering bearing. *Engineering Structures*, *300*, 117249. https://doi.org/10.1016/j.engstruct.2023.117249.

Wu, M., Ba, Z., & Liang, J. (2022). A procedure for 3D simulation of seismic wave propagation considering source-path-site effects: Theory, verification and application. *Earthquake Engineering & Structural Dynamics*, *51*(12), 2925–2955. https://doi.org/10.1002/eqe.3708.

Xiang, Q. Q., Li, Y. D., Wei, K., Wang, S., & Yao, C. (2019). Review of bridge foundation scour. *Journal of Southwest Jiaotong University*, *54*(2), 21–34. https://doi.org/10.3969/j.issn.0258-2724.20170373.

Ye, A. J., Zhang, X. G., & Liu, W. A. (2007). Effects of riverbed scouring depth on the seismic response of bridges on pile foundations. *China Civil Engineering Journal*, *3*, 58–62.

Zhang, Y. J., & Tien, I. (2022). Methodology to account for the impact of stress history in layered soils for seismic vulnerability assessment of scoured bridges. *Structure and Infrastructure Engineering*, *18*(5), 653–677. https://doi.org/10.1080/15732479.2020.1860096.

Zhang, Y., & Wu, G. (2019). Seismic vulnerability analysis of rc bridges based on kriging model. *Journal of Earthquake Engineering*, *23*(1–2), 242–260. https://doi.org/10.1080/13632469.2017.1323040.

Authors and Affiliations

Jianfeng Li[1,2] · Mengmeng Jin[3] · Junbo Chen[3,4] · Guojun Wang[5] · Yufeng Wang[1] · Huihui Yan[6] · Zucan Weng[7] · Zhigang Huang[8] · Hui Ai[9] · Li Wu[1]

✉ Li Wu
wuli7809@126.com

1 Faculty of Engineering, China University of Geosciences, Wuhan 430000, China

2 Fujian Branch, Hainan Cloud Spacetime Information Technology Co., Ltd, Danzhou 571700, China

3 Cavite State University, Indang 4100, Philippines

4 Zhejiang Industry &Trade Vocational College, Wenzhou 325000, China

5 Guangzhou Expressway Co., Ltd., Guangzhou 510000, China

6 Wenzhou Data Management and Development Group Co., Ltd., Wenzhou 325000, China

7 Fuzhou Planning & Design Research Institute Grop Co., Ltd., Fuzhou 350001, China

8 Fuzhou Water Pingtan Water Diversion & Develsopment Co., Ltd., Fuzhou 350001, China

9 Nuclear Industry Jingxiang Construction Group Co., Ltd., Huzhou 313000, China